

## Recent electroweak measurements from the H1 and ZEUS experiments

Arafat Gabareen Mokhtar  
*Tel Aviv University,*  
*Tel Aviv, Israel*  
*for the H1 and ZEUS collaborations*  
*Email: gabareen@mail.desy.de*



Neutral-current (NC) and charged-current (CC) deep inelastic scattering (DIS) reactions have been studied in  $e^+p$  and  $e^-p$  collisions using the H1 and ZEUS detectors at HERA I. Following the upgrade of the HERA accelerator, the HERA II program recently started with the first data in  $e^+p$  scattering with longitudinally polarised positrons. In this paper, a summary of the electroweak results from HERA I and the first measurement of the cross section for  $e^+p$  CC DIS at a longitudinal polarisation value of 33% from the ZEUS collaboration are presented.

### 1 HERA I

At HERA<sup>1</sup>, a proton beam of 920 GeV<sup>a</sup> collides with an electron or positron<sup>b</sup> beam of 27.5 GeV. The electron-proton ( $ep$ ) interactions proceed via  $\gamma$  and  $Z^0$ - exchange in the neutral current (NC) reaction, or via  $W^\pm$  exchange in the charged current (CC) interaction. The description of events is usually given in terms of the  $ep$  center of mass energy squared,  $s$ , and two out of three Lorentz invariant quantities,  $Q^2$ : the absolute value of the invariant mass squared of the exchanged particle,  $x$ : the fraction of the proton momentum carried by the struck quark, and  $y$ ; the fractional energy transferred to the proton in its rest frame. These variables are related through  $Q^2 = sxy$ , if the masses of the electron and the proton are neglected.

<sup>a</sup>Until 1998, the energy of the proton beams were 820 GeV.

<sup>b</sup>In the following, for simplicity we will denote as electron the charged lepton, independent of whether it is an  $e^+$  or an  $e^-$ , unless otherwise stated.

### 1.1 Neutral current

The double differential NC cross section for the reaction  $ep \rightarrow eX$  with longitudinally unpolarised electron is given by

$$\frac{d^2\sigma_{Born}^{NC}(e^\pm p)}{dx dQ^2} = \frac{2\pi\alpha^2}{xQ^4} \left[ Y_+ F_2^{NC}(x, Q^2) \mp Y_- xF_3^{NC}(x, Q^2) \right], \quad (1)$$

where  $\alpha$  denotes the fine-structure constant and  $Y_\pm = 1 \pm (1-y)^2$ . The contribution of the longitudinal structure function was neglected. The structure function  $F_2^{NC}$  can be divided into three terms, due to electromagnetic interactions, to the interference between the photon and  $Z^0$  exchange, and pure  $Z^0$  exchange<sup>2</sup>, such that

$$F_2^{NC} \equiv \mathbf{F}_2^{em} - v_e \frac{\kappa Q^2}{Q^2 + M_{Z^0}^2} \mathbf{F}_2^{\gamma Z^0} + (v_e^2 + a_e^2) \left( \frac{\kappa Q^2}{Q^2 + M_{Z^0}^2} \right)^2 \mathbf{F}_2^{Z^0}, \quad (2)$$

where  $\kappa \equiv 4 \frac{M_W^2}{M_{Z^0}^2} (1 - \frac{M_W^2}{M_{Z^0}^2})$ ,  $M_W$  ( $M_{Z^0}$ ) is the  $W^\pm$  ( $Z^0$ ) boson mass, and  $v_e$  and  $a_e$  are the NC couplings of the  $Z^0$  to the electron. The couplings of the quarks are contained in the respective  $F_2^{NC}$  structure functions ( $F_2^{em}, F_2^{\gamma Z^0}$  and  $F_2^{Z^0}$ ).

The parity violating structure function,  $xF_3^{NC}$ , contains two terms: one due to the interference between photon and  $Z^0$  exchange amplitudes and a term due to pure  $Z^0$  exchange,

$$xF_3^{NC} \equiv -a_e \frac{\kappa Q^2}{Q^2 + M_{Z^0}^2} \mathbf{xF}_3^{\gamma Z^0} + 2v_e a_e \left( \frac{\kappa Q^2}{Q^2 + M_{Z^0}^2} \right)^2 \mathbf{xF}_3^{Z^0}. \quad (3)$$

When  $\frac{Q^2}{M_{Z^0}^2} \ll 1$ , the NC process is dominated by photon exchange. When  $Q^2$  becomes of the order of  $M_{Z^0}^2$ , the contribution from the interference and pure  $Z^0$  exchange is non-negligible.

Fig. 1, shows the NC cross section as a function of  $Q^2$  for  $e^+p$  and  $e^-p$  scattering as measured by the ZEUS<sup>3</sup> and H1<sup>4</sup> experiments. The NC cross section for  $e^+p$  is equal to that of  $e^-p$  at low  $Q^2$  because in this kinematic region the electromagnetic interaction dominates. The structure function  $xF_3^{NC}$  has a negative contribution to the cross section in case of  $e^+p$  and a positive one in case of  $e^-p$ . This can be observed in eq. 1, where at high  $Q^2$  the difference between the  $e^+p$  and  $e^-p$  NC cross section becomes noticeable. Measurements by H1 and ZEUS are in a good agreement with expectations of the Standard Model (SM), calculated with the CTEQ6D<sup>5</sup> parameterisation of parton distribution functions (PDFs) in the proton.

The measurements of  $F_2^{em}$  at HERA I are shown in Fig. 2, where the values of  $F_2^{em}$  are plotted as a function of  $Q^2$  for fixed values of  $x$ . Strong scaling violations are observed, especially at low values of  $x$ . This is the manifestation of the presence of a large gluon density in the proton. The observed scaling violations are well reproduced by the DGLAP<sup>6</sup> evolution of perturbative QCD.

The structure function  $xF_3^{NC}$  can be determined from the difference of  $e^\pm p$  cross sections,

$$xF_3 = \frac{xQ^4}{4\pi\alpha^2 Y_-} \left[ \frac{d^2\sigma(e^-p)}{dx dQ^2} - \frac{d^2\sigma(e^+p)}{dx dQ^2} \right]. \quad (4)$$

The  $xF_3^{NC}$  extracted at HERA I<sup>7, 8</sup> is shown in Fig. 3, as a function of  $x$  for different  $Q^2$  bins. Within uncertainties, the measured  $xF_3^{NC}$  is in agreement with expectations obtained using the CTEQ6D PDFs.

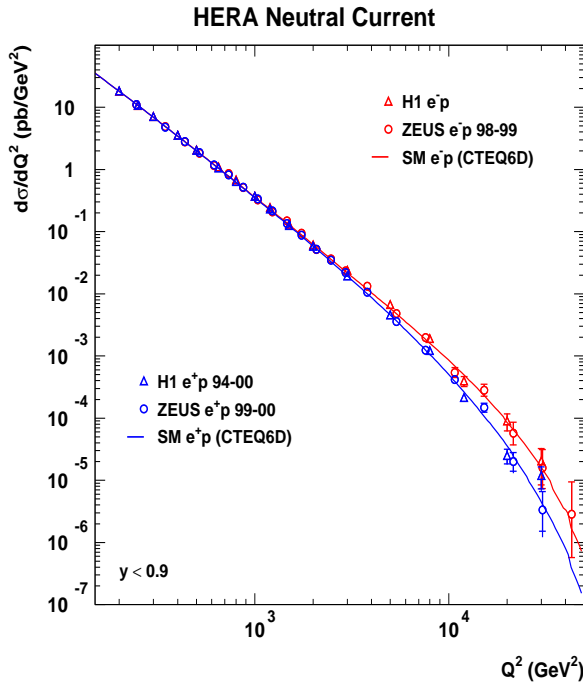


Figure 1: The NC cross section versus  $Q^2$  for  $e^+p$  and  $e^-p$  interactions as measured by the H1 and ZEUS experiments.

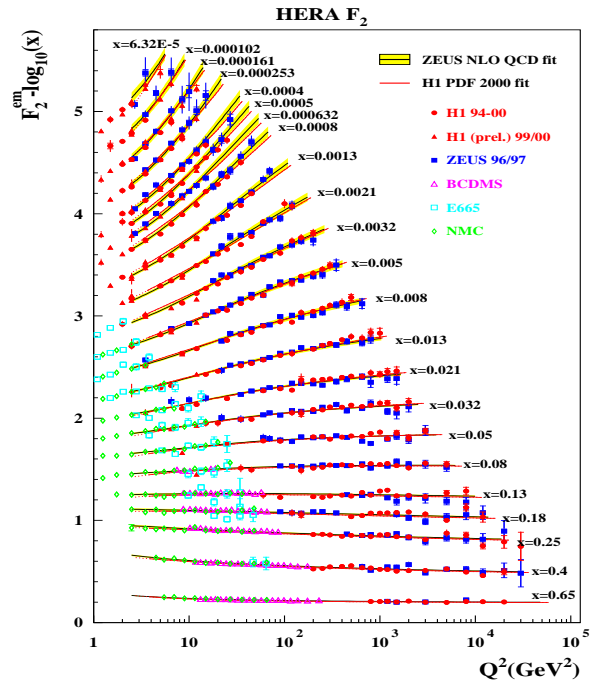


Figure 2: The structure function  $F_2^{em}$  versus  $Q^2$  at fixed values of  $x$  compared to a fit based on DGLAP evolution equations.

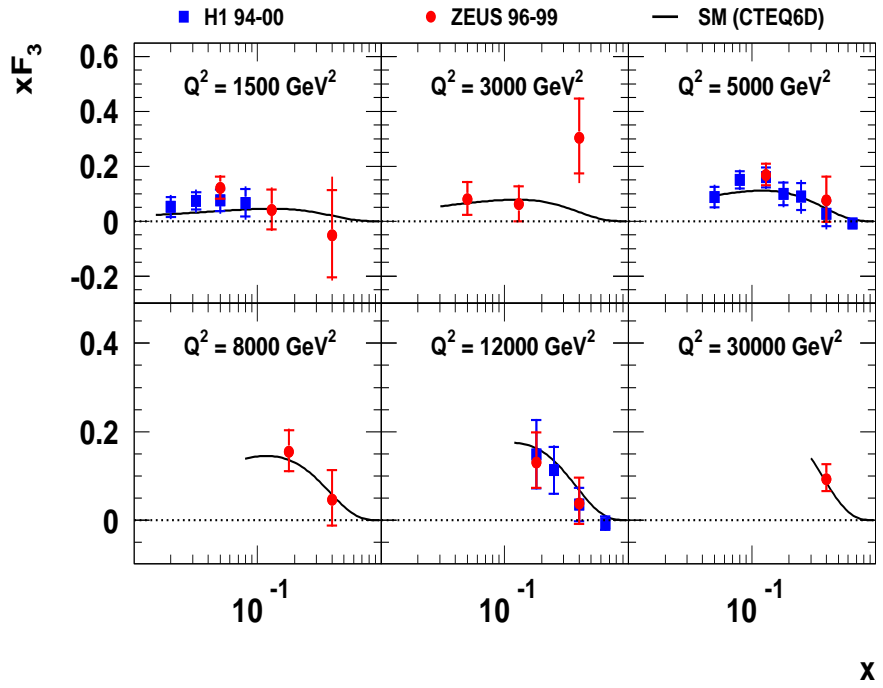


Figure 3: The structure function  $x F_3$  versus  $x$  at different values of  $Q^2$  as obtained by the H1 and ZEUS experiments.

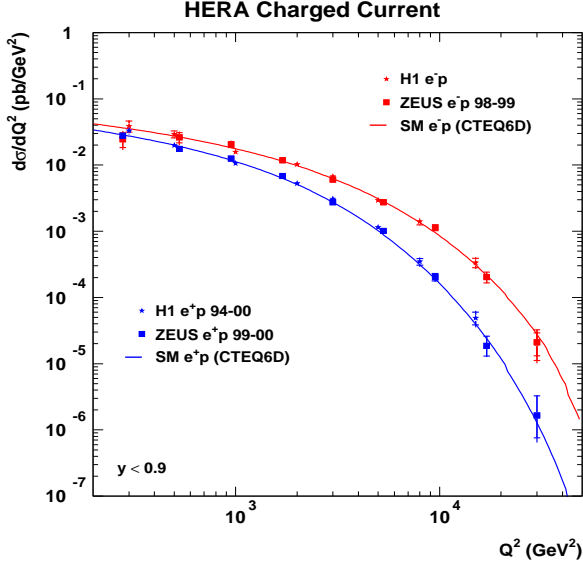


Figure 4: The CC cross section for  $e^+p$  and  $e^-p$  interactions versus  $Q^2$ .

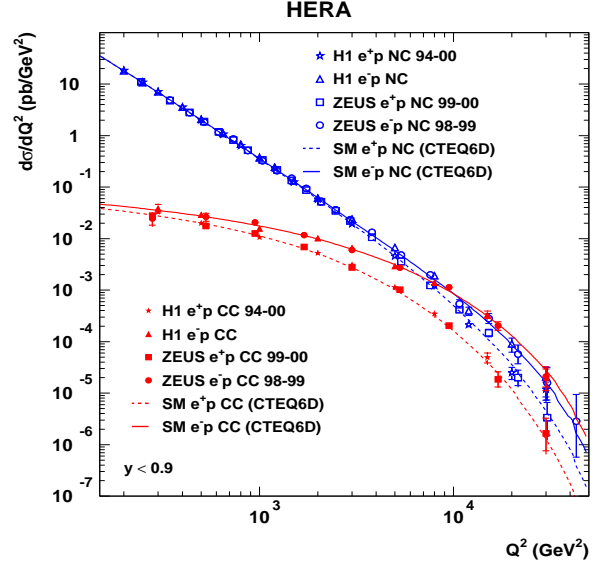


Figure 5: The NC and CC cross sections for  $e^+p$  and  $e^-p$  interactions versus  $Q^2$ .

## 1.2 Charged current

The cross sections for CC deep inelastic scattering with longitudinally unpolarised leptons on protons,  $e^-p \rightarrow \nu_e X$  and  $e^+p \rightarrow \bar{\nu}_e X$ , are given by

$$\frac{d^2\sigma_{Born}^{CC}(e^+p)}{dx dQ^2} = \frac{G_\mu^2}{2\pi} \left( \frac{M_W^2}{Q^2 + M_W^2} \right)^2 \cdot \left[ (\bar{u} + \bar{c}) + (1-y)^2(d+s) \right], \quad (5)$$

$$\frac{d^2\sigma_{Born}^{CC}(e^-p)}{dx dQ^2} = \frac{G_\mu^2}{2\pi} \left( \frac{M_W^2}{Q^2 + M_W^2} \right)^2 \cdot \left[ (u+c) + (1-y)^2(\bar{d} + \bar{s}) \right], \quad (6)$$

where  $G_\mu$  is the Fermi coupling constant and  $M_W$  is the W boson mass. The third quarks generation was neglected in eq. (5) and in eq. (6). At high  $x$  values, one can safely ignore the sea quarks and assume that the proton is dominated by the valence quarks. Under this assumption, the  $e^+p$  CC cross section is proportional to  $(1-y)^2 d$ , while the  $e^-p$  CC cross section is proportional to  $u$ . Since the  $u$  quark dominates in the proton, the  $e^-p$  CC cross section is higher than the  $e^+p$  CC cross section. This is shown in Fig. 4, where the  $e^+p$  and  $e^-p$  CC cross section is plotted as a function of  $Q^2$ . A good agreement between the two experiments, H1 and ZEUS, is observed and the measured values are well reproduced by the SM calculations based on the CTEQ6D PDFs.

## 1.3 EW unification

A comparison of NC and CC  $e^\pm p$  cross sections as a function of  $Q^2$  is shown in Fig. 5. Around  $Q^2 \sim 10^4$  GeV<sup>2</sup>, the CC and NC cross sections become equal. Since the NC cross section is dominated by electromagnetic component this equality can be interpreted as a manifestation of electroweak unification.

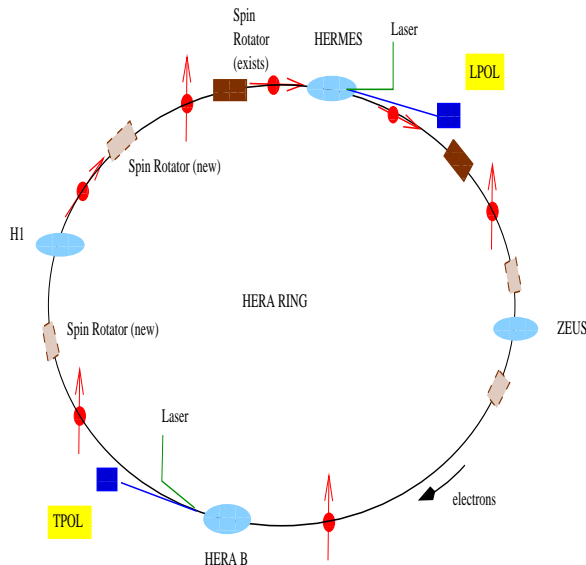


Figure 6: A schematic picture of HERA II after the upgrade.

## 2 HERA II

### 2.1 HERA II upgrade

In order to study in detail the properties of deep inelastic scattering at high  $Q^2$ , the HERA accelerator was upgraded to deliver a five fold increase in luminosity and longitudinally polarised lepton beams<sup>c</sup>. To meet the challenge, the H1 and the ZEUS detectors were upgraded: a new inner silicon vertex detector was installed at ZEUS to increase the efficiency of the vertex reconstruction; an extension of the inner silicon detectors in H1 was done; new forward tracking detectors were installed in both H1 and ZEUS detectors; luminosity detectors were modified in H1 and ZEUS; a new track trigger was added in H1<sup>9</sup>.

In order to measure the polarisation at HERA II, two independent polarimeters are in use based on different measurement methods, the longitudinal polarimeter (LPOL) and the transverse polarimeter (TPOL). The LPOL is located near the HERMES experiment and was in use during the HERA I run period. The TPOL was upgraded and is to be used in the HERA II run period. In addition, spin rotators were installed so that both H1 and ZEUS have now access to longitudinally polarised  $e^\pm$  beams. The location of the polarimeters and the spin rotators is shown in Fig. 6.

### 2.2 Charged current and polarisation

The Standard Model predicts that the charged current cross section for collisions of polarised electrons with protons is proportional to  $1 \pm P$ , where  $P$  is the longitudinal polarisation of electrons. In other words, the SM predicts that the CC cross section for fully right-handed electrons (left-handed positrons) with colliding protons is zero.

The first measurement of  $e^+p$  CC cross section with  $P = 33 \pm 2\%$  and with integrated luminosity of  $6.6 \text{ pb}^{-1}$ , has been made by the ZEUS collaboration. The total CC cross section was measured for  $Q^2 > 400 \text{ GeV}^2$ , and shows a significant rise of the cross section relative to the unpolarised case from HERA I, as can be seen in Fig. 7. In the lower part of Fig. 7, the ratio of polarised to unpolarised cross section is shown. The increase of the cross section is well reproduced by the SM expectations.

<sup>c</sup>HERA I had provided longitudinal polarised lepton beam to the fixed target experiment, HERMES.

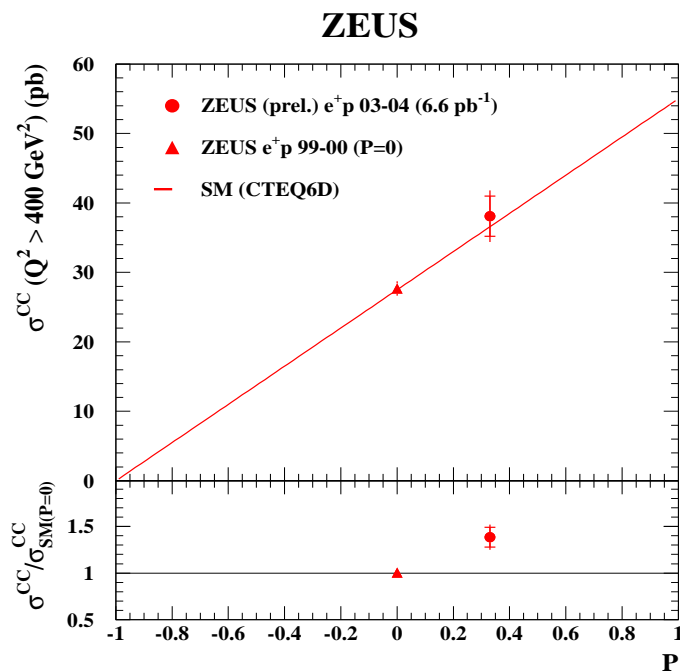


Figure 7: Upper: the total CC DIS cross section for  $e^+p$  scattering plotted as a function of the polarisation of the incoming lepton beam,  $P$ . Lower: the ratio of the polarised to unpolarised cross section as a function of the polarisation.

### 3 Acknowledgements

This work was partially supported by the Björn Wiik World Laboratory Scholarship Programme at DESY, the MINERVA Foundation, the Israel Science Foundation (ISF) and the Israeli Ministry of Science.

### 4 Bibliography

1. HERA, “A proposal for a large electron-proton colliding beam facility at DESY”, DESY HERA 81-10.
2. M. Klein and T. Riemann, *Z. Phys.* **C 24**, 151 (1984).
3. ZEUS Collab., S. Chekanov *et al.*, “High- $Q^2$  neutral current cross sections in  $e^+p$  deep inelastic scattering at  $\sqrt{s} = 318\text{-GeV}$ ,” arXiv:hep-ex/0401003.  
ZEUS Collab., S. Chekanov *et al.*, *Eur. Phys. J. C* **28**, 175 (2003).  
ZEUS Collab., S. Chekanov *et al.*, *Eur. Phys. J. C* **21**, 443 (2001).  
ZEUS Collab., J. Breitweg *et al.*, *Eur. Phys. J. C* **11**, 427 (1999).
4. H1 Collab., C. Adloff *et al.*, *Eur. Phys. J. C* **13**, 609 (2000).  
H1 Collab., C. Adloff *et al.*, *Eur. Phys. J. C* **19**, 269 (2001).  
H1 Collab., S. Aid *et al.*, *Phys. Lett. B* **379**, 319 (1996).
5. S. Kretzer, H. L. Lai, F. I. Olness and W. K. Tung, *JHEP* **7**, 12 (2002).
6. V. N. Gribov and L. N. Lipatov, *Sov. J. Nucl. Phys.* **15**, 438 (1972).  
V. N. Gribov and L. N. Lipatov, *Sov. J. Nucl. Phys.* **15**, 675 (1972).  
Yu.L. Dokshitzer, *Sov. Phys. JETP* **46**, 641 (1977).  
G. Altarelli and G. Parisi, *Nucl. Phys.* **B 126**, 298 (1977).
7. ZEUS Collab., S. Chekanov *et al.*, *Eur. Phys. J. C* **28**, 175 (2003)
8. H1 Collab., C. Adloff *et al.*, *Eur. Phys. J. C* **19**, 269 (2001)
9. A. Mehta, HERA upgrade and prospects, *ACTA Phys. Pol.* **B 33**, 3937 (2002).